

DEUTSCHES ELEKTRONEN-SYNCHROTRON **DESY**

DESY 86-043
April 1986



EXCLUSIVE PRODUCTION OF PROTON-ANTIPROTON PAIRS IN PHOTON-PHOTON COLLISIONS

JADE Collaboration

ISSN 0418-9833

NOTKESTRASSE 85 · 2 HAMBURG 52

DESY behält sich alle Rechte für den Fall der Schutzrechtserteilung und für die wirtschaftliche Verwertung der in diesem Bericht enthaltenen Informationen vor.

DESY reserves all rights for commercial use of information included in this report, especially in case of filing application for or grant of patents.

**To be sure that your preprints are promptly included in the
HIGH ENERGY PHYSICS INDEX ,
send them to the following address (if possible by air mail) :**

**DESY
Bibliothek
Notkestrasse 85
2 Hamburg 52
Germany**

Exclusive Production of Proton-Antiproton Pairs in Photon-Photon Collisions

JADE Collaboration

W. Bartel, L. Becker, D. Cords⁽¹⁾, R. Felst, D. Haidt, G. Knies, H. Krehbiel, P. Laurikainen⁽²⁾,
N. Magnussen⁽³⁾, R. Meinke, B. Naroska, J. Olsson, D. Schmidt⁽³⁾, P. Steffen
Deutsches Elektronen-Synchrotron DESY, Hamburg, Germany

G. Dietrich, J. Hagemann, G. Heinzelmann, H. Kado, K. Kawagoe⁽⁴⁾, C. Kleinwort, M. Kuhlen,
A. Petersen⁽¹⁾, R. Ramcke, U. Schneekloth, G. Weber
II. Institut für Experimentalphysik der Universität Hamburg, Germany

K. Ambrus, S. Bethke, A. Dieckmann, E. Elsen, J. Heintze, K.-H. Heilenbrand, S. Komamiya,
J. von Krogh, P. Lennert, H. Matsumura, H. Rieseberg, J. Spitzer, A. Wagner
Physikalisches Institut der Universität Heidelberg, Germany

C.K. Bowdery, A.J. Finch, F. Foster, G. Hughes, J.M. Nye
University of Lancaster, England

J. Allison, A.H. Ball⁽⁵⁾, R.J. Barlow, J. Chrin, I.P. Duerdoth, T. Greenshaw, F.K. Loebinger,
A.A. Macbeth, H.E. Mills, P.G. Murphy, K. Stephens, P. Warming
University of Manchester, England

R.G. Glasser, P. Hill, J.A.J. Skard, S.R. Wagner⁽⁶⁾, G.T. Zorn
University of Maryland, College Park, Maryland, USA

S.L. Cartwright, D. Clarke, R. Marshall, R.P. Middleton,
Rutherford Appleton Laboratory, Chilton, England

T. Kawamoto, T. Kobayashi, H. Takeda, T. Takeshita, S. Yamada
International Center for Elementary Particle Physics, University of Tokyo, Japan

⁽¹⁾ Now at SLAC, California, USA

⁽²⁾ University of Helsinki, Helsinki, Finland

⁽³⁾ Universität-Gesamthochschule Wuppertal, Germany

⁽⁴⁾ Deutscher Akademischer Austauschdienst (DAAD) Fellow

⁽⁵⁾ Now at University of Maryland, College Park, Md., USA

⁽⁶⁾ Now at University of Colorado, Boulder, Co., USA

ABSTRACT

Total and differential cross sections for exclusive production of proton-antiproton pairs in photon-photon collisions have been measured using the JADE detector at PETRA. The total cross section in the c. m. angular range $|\cos\theta^*| < 0.6$ reaches a maximum value of 3.8 nb for a $\gamma\gamma$ invariant mass of $W_{\gamma\gamma} = 2.25$ GeV, and decreases rapidly for higher values of $W_{\gamma\gamma}$. In the range $2.0 \text{ GeV} < W_{\gamma\gamma} < 2.6 \text{ GeV}$ the angular distribution is not isotropic. The nucleons are preferentially emitted at large angles to the collision axis.

In recent years perturbative QCD calculations have successfully been applied to describe many features of large-momentum-transfer inclusive scattering processes. Also in exclusive hadron scattering, e.g. in experimental data on nucleon-nucleon scattering, Compton scattering, photoproduction, and the pion and proton form factors, one finds cross sections in remarkably good agreement with the power-law energy dependence predicted [1] from QCD, for momentum transfers $|t| > 5 \text{ GeV}^2$. Recent data [2] on meson pair production in photon-photon collisions, however, show good agreement with a perturbative QCD calculation [3] even for $|t|$ -values as low as 1.5 GeV^2 . Cross sections for proton-antiproton production in $\gamma\gamma$ collisions have also been calculated in perturbative QCD [4]. The only published experimental result [5] for this process reaches $|t|$ -values of up to 4 GeV^2 , and gives cross sections which are one to two orders of magnitude larger than the QCD prediction.

In this paper we present a new measurement of the cross sections for the process $\gamma\gamma \rightarrow p\bar{p}$ via the reaction $e^+e^- \rightarrow e^+e^-p\bar{p}$. The data were taken with the JADE detector at the PETRA e^+e^- storage ring. The data sample used for determining the cross sections was collected during the period from 1980 to 1984, and corresponds to an integrated e^+e^- luminosity of 59.3 pb^{-1} at beam energies around 17.4 GeV , and an additional 24.2 pb^{-1} at around 21.9 GeV .

A description of the JADE detector can be found elsewhere [6]. Essential components for the present measurement were the central jet chamber (a cylindrical drift chamber) and the 42 time-of-flight (TOF) counters, covering the full azimuth around the jet chamber. The jet chamber provides, besides tracking information, up to 48 samples of the specific energy loss dE/dx per track, giving an overall dE/dx resolution of about 6 % in the events described here. (The mean number of dE/dx samples per track was 39.) The TOF counters, with a time resolution of ≈ 350 picoseconds, were used in the event trigger, and also in the rejection of background events.

The reaction $e^+e^- \rightarrow e^+e^-p\bar{p}$ is expected to proceed predominantly via two quasi-real photons, i.e. photons with small four-momentum squared. This leads to an event configuration in which the $\gamma\gamma$ system has low transverse momentum relative to the e^+e^- beam axis. The electron and positron will therefore mostly go undetected, due to their small scattering angles, and the acoplanarity angle for the $p\bar{p}$ pair (the angle between the two planes defined by each of the two nucleon momentum vectors and the e^+e^- beam axis) will be small. This coplanarity of the nucleon pair was utilized in the event trigger. The trigger required signals in two TOF counters, located opposite each other to within ± 3 counters, in coincidence with two tracks pointing to these counters in the central drift chamber. In order to avoid high trigger rates of spurious events where the coplanar trigger condition had been set by random noise hits in the TOF counters, the trigger allowed no more than 4 counters altogether to have a signal. During some running periods with high background conditions a maximum of 3 counters was allowed. In very coplanar events (within ± 1 counter) up to 6 TOF counters were allowed to have a signal, and a maximum of 4 counters during the high background periods.

The candidate events for the reaction $e^+e^- \rightarrow e^+e^-p\bar{p}$ were selected via the following criteria:

- i) A minimum of two tracks was required, each with a momentum between 0.4 and 1.0 GeV/c. The upper limit was chosen to ensure a clean identification of the particle by the dE/dx measurement. The lower limit reduces uncertainties due to nuclear absorption and energy loss in the beam pipe and inner pressure tank wall.
- ii) Each track, when extrapolated to the interaction region, was required to pass within 2 cm of the average e^+e^- interaction point, measured in the plane transverse to the e^+e^- beams, and within 10 cm measured along the beams. Each event should have exactly two such "good" tracks. The average interaction point was determined independently from large-angle Bhabha scattering events.
- iii) The two particles should be identified as a proton and an antiproton, respectively. For this purpose the dE/dx information from the central jet chamber was used. The χ^2 for each particle hypothesis was calculated by a method which minimizes χ^2 , taking into account the errors in both the dE/dx and the momentum measurements. The momentum error for nucleons in the selected

momentum range is dominated by multiple scattering, and varied between 8 % and 13 %. The resulting probability distribution of χ^2 (with 1 degree of freedom) turns out to be flat for a clean sample of one type of particles, as expected. The value of χ^2 for the p/\bar{p} hypothesis was required to be less than 3. This corresponds to an acceptance of approximately 92 % of all genuine proton and antiproton tracks.

- iv) Several events of the type $e^+e^- \rightarrow e^+e^-e^+e^-$ were left in the data sample after the above cuts, since electrons and protons have approximately the same value for dE/dx at momenta near 1 GeV/c. These events were effectively removed by requiring that the energy deposited by the positive particle in the lead glass shower counters should not exceed $0.5cp$ for momenta $p > 0.5$ GeV/c. (A test on shower energy for the negative particle could not be used, since the annihilation of the antiproton deposits an energy in the lead glass of the same magnitude as that from a 1 GeV electron.)
- v) In order to reject events with additional, undetected final state particles, as well as background events from beam-gas interactions, the total transverse momentum of the $p\bar{p}$ system with respect to the e^+e^- beam axis was required to be less than 200 MeV/c, after the momentum of each track had been corrected for energy loss in the beam pipe and the inner pressure tank wall. For the same reasons the acoplanarity angle was required to be less than 7° . These two cuts restricted the momentum transfer q^2 of the colliding, virtual photons to $|q^2| < 0.05$ (GeV/c) 2 , with an average value of $\langle q^2 \rangle = -1.5 \cdot 10^{-3}$ (GeV/c) 2 , as determined from a Monte Carlo simulation (discussed later).
- vi) An important remaining background consisted of events where a proton would traverse the entire detector, passing close enough to the interaction point to simulate a genuine $p\bar{p}$ event. These protons appeared mostly to be emitted in nuclear reactions caused by particles coming from stray beam-particle interactions at points outside the detector. (In some of these events the incident particle, usually a pion, was clearly seen in the central detector.) Cuts on time-of-flight, in conjunction with cuts on collinearity and vertex position, removed all but a few such events.
- vii) Finally, all events were examined individually, and the few remaining events with a proton traversing the whole detector, along with some background events of the type $e^-e^- \rightarrow e^+e^-e^+e^-$, were removed.

A total of 57 events passed all of the cuts described above. The distribution of the total transverse momentum squared ($|\sum \vec{p}_\perp|^2$) of the $p\bar{p}$ system is shown in Fig. 1a, and Fig. 1b shows the acoplanarity distribution. An additional 5 $\gamma\gamma \rightarrow p\bar{p}$ events from an earlier running period (which were not used for determining the cross sections, due to uncertainties in the trigger efficiency), as well as one event where one of the nucleons had a momentum slightly below the 0.4 GeV/c cut, are included in these figures, bringing the total number of events up to 63 (shown as triangles in the figures). Both distributions show a strong peak at zero, as expected for exclusive $\gamma\gamma \rightarrow p\bar{p}$ events.

After correction of the $p\bar{p}$ momenta for energy loss in the beam pipe and inner tank wall, and extrapolation of the tracks to a vertex point, the invariant mass $W_{\gamma\gamma}$ of each $p\bar{p}$ pair was calculated. The resulting mass distribution (again including the 6 additional events) is shown in Fig. 2 (dashed histogram). The mass resolution in this region is about 25 MeV/c 2 .

In order to calculate cross sections for the process $\gamma\gamma \rightarrow p\bar{p}$, simulated events were generated via a Monte Carlo computer program [7], passed through a program simulating the response of the JADE detector, and finally subjected to the same selection criteria as the real events. The events were generated according to

$$d\sigma(e^+e^- \rightarrow e^+e^-p\bar{p}) = F(\tau) \frac{d\sigma_{\gamma\gamma}}{d\Omega} d\tau d\Omega', \quad (1)$$

where $d\tau$ is the differential invariant phase space element for the scattered e^+e^- pair, $F(\tau)$ contains the QED factors for the production of a system of two transversely polarized, virtual photons [8],

while the solid angle element $d\Omega' = d\phi' d(\cos\theta')$ refers to the direction of the final state proton in the $\gamma\gamma$ center-of-mass system. (θ' is the polar angle with respect to the e^+ beam direction.) In the Monte Carlo simulation the events were generated with a constant cross section $\sigma_{\gamma\gamma}$, and with an isotropic distribution of the nucleons in the $\gamma\gamma$ c. m. system.

50 000 events were generated and tracked at each of the two beam energies. The detector simulation included the effects of energy loss, nuclear absorption and large-angle scattering¹, known detector inefficiencies, and resolution. A total of 3 117 (3.1 %) of the Monte Carlo events passed all of the cuts in the data selection.

Due to the longitudinal boost of the $\gamma\gamma$ -system the detection efficiency is sensitively dependent on the $\cos\theta'$ distribution of the $p\bar{p}$ system, particularly for low values of $W_{\gamma\gamma}$. In order to minimize uncertainties coming from the a priori unknown $\cos\theta'$ distribution the Monte Carlo events (and the data) were therefore grouped in bins of both $W_{\gamma\gamma}$ and $z = \cos\theta'$. Since the differential distribution of the N (isotropic) Monte Carlo events is simply $\frac{dN}{dz} = \frac{N}{2}$, the differential and total cross sections are then given by

$$\frac{d\sigma_{\gamma\gamma}(W_{\gamma\gamma}, z_i)}{dz} = \frac{N}{2\mathcal{L}I} \cdot \frac{N_{\Delta W, \Delta z}^{\text{obs}}}{N_{\Delta W, \Delta z}^{\text{MC}}} \cdot \delta \quad (2)$$

and

$$\sigma_{\gamma\gamma}(W_{\gamma\gamma}) = \sum_{z_i \in [z_{\min}, z_{\max}]} \frac{d\sigma_{\gamma\gamma}(W_{\gamma\gamma}, z_i)}{dz} \Delta z, \quad (3)$$

where (2) gives the differential cross section in the bin Δz around z_i , averaged over the $W_{\gamma\gamma}$ interval ΔW , while (3) gives the total $\gamma\gamma \rightarrow p\bar{p}$ cross section, averaged over the interval ΔW around W , and summed over the $\cos\theta'$ range from z_{\min} to z_{\max} . \mathcal{L} is the integrated e^+e^- luminosity. I is the right-hand side of Eq. (1), integrated by the Monte Carlo program over the $W_{\gamma\gamma}$ -range 1.9 GeV to 2.7 GeV, with $\frac{d\sigma_{\gamma\gamma}}{d\Omega'}$ set equal to $\frac{1}{4\pi}$. $N_{\Delta W, \Delta z}^{\text{MC}}$ is the number of accepted Monte Carlo events in the interval defined by ΔW and Δz , and $N_{\Delta W, \Delta z}^{\text{obs}}$ is the number of observed events in this same interval. The quantity δ contains corrections for inefficiencies not simulated by the Monte Carlo program. These include effects of the χ^2 cut for dE/dx identification (a 16 % loss), gaps between the TOF counters (2 % loss), and some corrections to the Monte Carlo simulation of the trigger efficiency, described below.

In most of the events the annihilation of the antiproton in the outer pressure tank wall or in the lead glass caused signals in several TOF counters near the annihilation point. In 11 of the 57 $p\bar{p}$ events the coplanar trigger condition had been satisfied by one of these accidental hits, and not by the antiproton itself. These were mostly events where the nucleon transverse momenta were too low for the direct hits to meet the coplanar trigger requirement. In order to deal only with events for which the trigger efficiency was well understood, all of these accidentally triggered events were removed from the sample. Furthermore, in order to avoid hits in inefficient regions of the TOF counters, the polar angle of both nucleons with respect to the e^+ beam direction was restricted to $|\cos\theta| < 0.8$.

41 events remained after this selection. Their distribution in transverse momentum and acoplanarity is shown in Figs. 1a and 1b (open circles). Good agreement is seen with the distributions for the Monte Carlo simulated events (solid histogram). The invariant mass ($W_{\gamma\gamma}$) distribution of these final 41 events is shown in Fig. 2 (solid histogram). The elimination of events which accidentally set the coplanar trigger has reduced the acceptance for $\gamma\gamma \rightarrow p\bar{p}$ events most strongly in the region of low invariant mass, as could be expected, but the overall features of the mass distribution have remained the same.

¹The cross section for antiprotons on Al was interpolated from data on \bar{p} incident on carbon and copper, with $\sigma \propto A^{0.8}$ [9]. The cross section for protons was extrapolated from data on carbon and oxygen with $\sigma \propto A^{0.8}$ [10].

Due to the aforementioned trigger veto a correction for events lost through too many TOF hits from the \bar{p} annihilation and/or too many random noise hits had to be made. Calculated on the basis of the distribution of TOF signals in the triggered $\gamma\gamma \rightarrow p\bar{p}$ events, extrapolated into the region vetoed by the trigger, and folded with the noise hits distributions for the relevant run periods (obtained from independently triggered events), this amounted to an average loss of 22 %. The resulting value of the correction factor δ was on average about 1.6 .

The cross section for $\gamma\gamma \rightarrow p\bar{p}$ in the range $|\cos\theta^*| < 0.6$ is shown in Fig. 3. It exhibits a pronounced maximum of 3.8 nb at a $\gamma\gamma$ invariant mass of about 2.25 GeV, a feature which is clearly seen also in the uncorrected mass distributions (Fig. 2), and rapidly decreases for higher $W_{\gamma\gamma}$ -values.

The errors shown in Fig. 3 are statistical only. The systematic errors are dominated by the uncertainty in the correction due to accidental TOF hits from the \bar{p} annihilation. Reasonable variations of the distribution used to correct for this changed the efficiency by ± 9 %. The systematic errors due to uncertainties in the luminosity measurement, corrections for nuclear absorption and energy loss, the cut on χ^2 for dE/dx, and possible contamination by events with additional, unobserved final state particles are all at the 3 % level or smaller. Added in quadrature, these errors give an overall systematic error of 11 %. An additional systematic error stems from the lack of knowledge of the form of the coupling between the photons and the proton-antiproton pair. Monte Carlo studies show that if a q^2 dependence in the form of a ρ -pole form factor were used instead of a constant¹ the calculated cross sections would be reduced by a few percent.

The differential cross section is shown in Fig. 4. One sees a clear preference in the data for the protons/antiprotons to be emitted at large angles to the e^+e^- beam directions in this mass range. With the data grouped in two $|\cos\theta^*|$ bins, also shown in Fig. 4, an isotropic cross section gives a fit with a probability of less than 0.1 % ($\chi^2/\text{D.O.F.} = 11.3/1$).

The curves on Figs. 3 and 4 show the theoretical cross sections calculated in perturbative QCD by G.R. Farrar et al.[12]. Their calculation was performed by taking the sum of all relevant quark amplitudes in the Born approximation, convoluted with a wave function for the nucleons which has been derived[13] from QCD sum rules and adjusted to give good agreement with data for $\psi \rightarrow p\bar{p}$ and for the nucleon form factors. It is clearly seen that the QCD prediction does not describe the data for $\gamma\gamma \rightarrow p\bar{p}$ in the (low) invariant mass range accessible to this experiment, either in angular dependence or in magnitude. The previously published experimental results by the TASSO group[5], which are consistent with our results, support this conclusion. It should be noted that the maximum value of the momentum transfer in the events included in the present analysis is only $|t|_{\text{max}} \simeq 2.5 \text{ GeV}^2$, and that the total cross section appears to approach the predicted level for the highest $p\bar{p}$ invariant masses included in this analysis.

In conclusion, the total and differential cross sections for the process $\gamma\gamma \rightarrow p\bar{p}$ have been measured and found consistent with a previous measurement by the TASSO collaboration. The total cross section reaches a maximum of 3.8 nb at $W_{\gamma\gamma} = 2.25 \text{ GeV}$, and then decreases rapidly with increasing $W_{\gamma\gamma}$. In the range 2.0 to 2.4 GeV in $W_{\gamma\gamma}$ the cross section is at least one order of magnitude higher than predicted by perturbative QCD. The angular distribution is not flat, but favors large p and \bar{p} emission angles relative to the beam axis.

We are indebted to the PETRA machine group and to the DESY Computer Center staff for their excellent support during the experiment and to all engineers and technicians of the collaborating institutions who have participated in the maintenance of the apparatus. Discussions with H. Kolanoski, who pointed out a normalization error, are gratefully acknowledged. This experiment was supported by the Bundesministerium für Forschung und Technologie, by the Ministry of Education, Science and Culture of Japan, by the UK Science and Engineering Research Council through the Rutherford

¹Preliminary results [11] from the PEP-9/PEP-4 collaboration indicate only a weak q^2 -dependence in the cross section for $\gamma\gamma \rightarrow p\bar{p}$.

REFERENCES

1. S.J. Brodsky and G.R. Farrar, Phys. Rev. Lett. **31** (1973), p. 1153.
S.J. Brodsky and G.R. Farrar, Phys. Rev. **D11** (1983), p. 1309.
V.A. Matveev, R.M. Muryadin, and A.V. Tavkhelidze, Lett. Nuovo Cimento **7** (1973), p. 719.
2. PLUTO Coll., Ch. Berger et al., Z. Phys. **C26** (1984), p. 199.
Mark II Coll., J. Smith et al., Phys. Rev. **D30** (1984), p. 851.
Mark II Coll., J. Boyer et al., Phys. Rev. Lett. **56** (1986), p. 207.
3. S.J. Brodsky and G.P. Lepage, Phys. Rev. **D24** (1981), p. 1808.
4. G.R. Farrar, E. Maina, and F. Neri, Rutgers Univ. preprint RU-84-13 (1984).
An earlier, less complete calculation which gives a significantly higher result can be found in:
P.H. Damgaard, Nucl. Phys. **B211** (1983), p. 434.
5. TASSO Coll., R. Brandelik et al., Phys. Lett. **130B** (1983), p. 449.
6. JADE Coll., W. Bartel et al., Phys. Lett. **88B** (1979), p. 171; Phys. Lett. **92B** (1980), p. 206;
Phys. Lett. **99B** (1981), p. 277.
7. S. Kawabata, Program Write-up, unpubl. (1982); Contribution to the parallel sessions, reported by J.H. Field, Proceedings of the IVth International Colloquium on Photon-Photon Interactions, Paris, 1981, p. 447.
8. G. Bonneau, M. Gourdin and F. Martin, Nucl. Phys. **B54** (1973), p. 573 (Eq. 29d).
9. R.J. Abrams et al., Phys. Rev. **D4** (1971), p. 3235.
10. P. Schwaller et al., Nucl. Phys. **A316** (1979), p. 317.
11. R. McNeil, Contribution to the parallel sessions, reported by H. Kück, Proceedings of the VIth International Workshop on Photon-Photon Collisions, Lake Tahoe, Calif., USA, 1984.
12. G.R. Farrar, Proceedings of the VIth International Workshop on Photon-Photon Collisions, Lake Tahoe, Calif., USA (1984).
G.R. Farrar, E. Maina, and F. Neri, Nucl. Phys. **B259** (1985), p. 702.
13. V.L. Chernyak and I.R. Zhitnitsky, Nucl. Phys. **B246** (1984), p. 52.

two angular bins used in the fit to an isotropic cross section (see text). The solid curve is the QCD prediction of ref. 11 using the nucleon wave function of ref. 12, scaled to a $W_{\gamma\gamma}$ value of 2.3 GeV.

FIGURE CAPTIONS

- Figure 1 a) The $|\sum \vec{p}_\perp|^2$ distribution of all 63 $p\bar{p}$ events (triangles) and of the restricted sample of 41 events used to calculate the cross sections (open circles). The histogram shows the distribution of the accepted Monte Carlo events, normalized to the restricted event sample in the lowest two bins. The arrow indicates the location of the cut applied to the data.
b) The acoplanarity distribution for the full and the restricted $p\bar{p}$ event samples. The symbols have the same meaning as in a). The Monte Carlo distribution shown (histogram) is normalized to the number of events in the restricted sample. The cut at 7° is indicated by an arrow.
- Figure 2 Uncorrected distribution of the invariant mass $W_{\gamma\gamma}$ for the complete event sample (dashed histogram) and for the restricted event sample (solid histogram).
- Figure 3 Total cross section for $\gamma\gamma \rightarrow p\bar{p}$ as a function of invariant mass $W_{\gamma\gamma}$ of the $\gamma\gamma$ system for $|\cos\theta^*| < 0.6$. The solid curve is the QCD cross section calculated from ref. 11.
- Figure 4 Differential cross section for $\gamma\gamma \rightarrow p\bar{p}$ as a function of $|\cos\theta^*|$ (solid circles), where θ^* is the polar angle of the proton in the $\gamma\gamma$ c.m. system. The dashed histogram shows the mean value in the

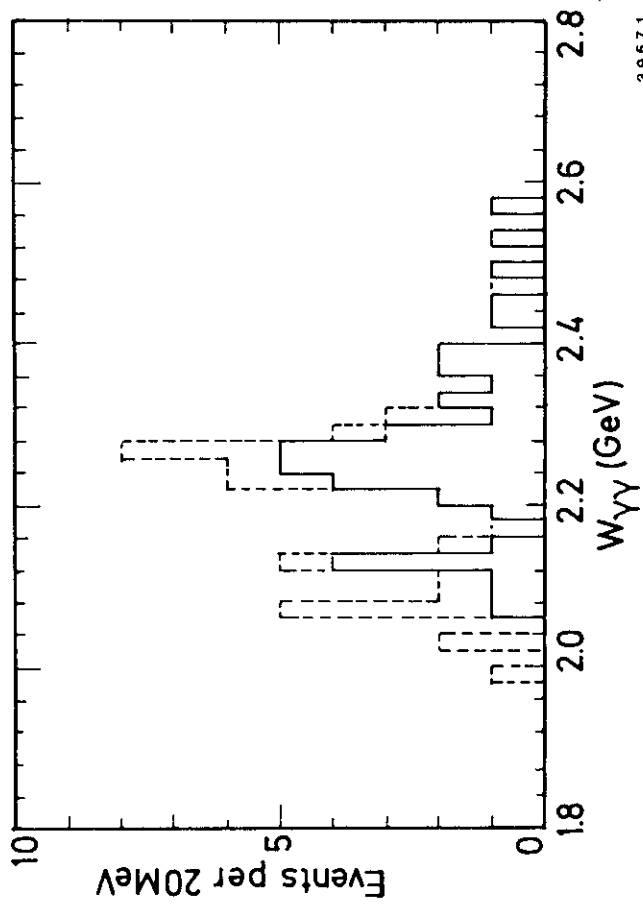


Fig.2

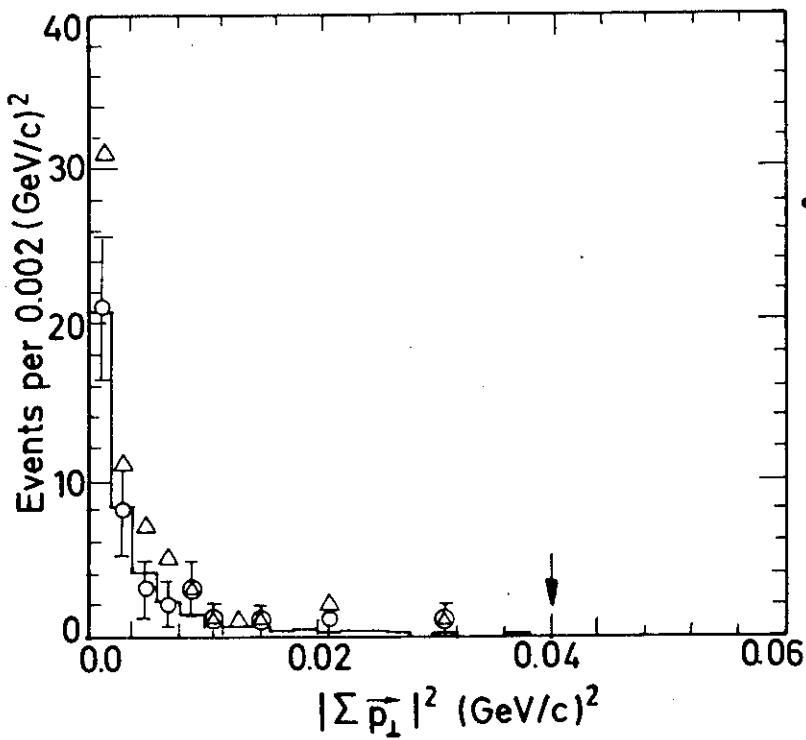


Fig.1a

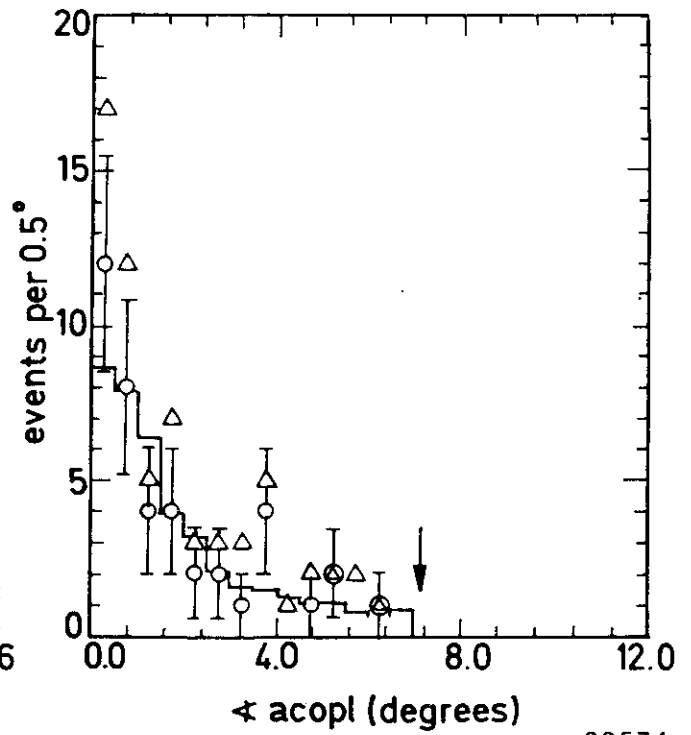


Fig.1b

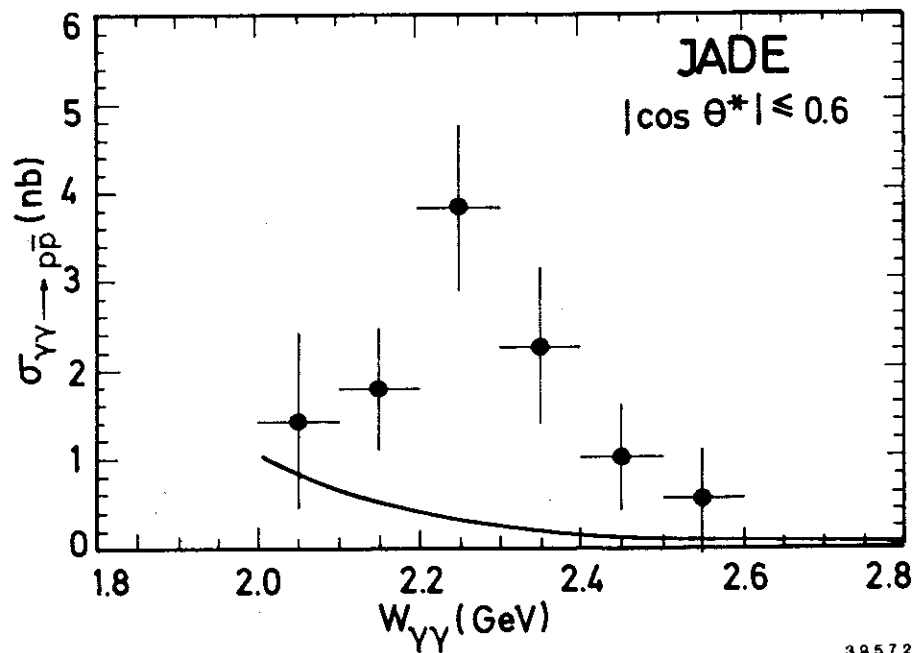


Fig. 3

39572

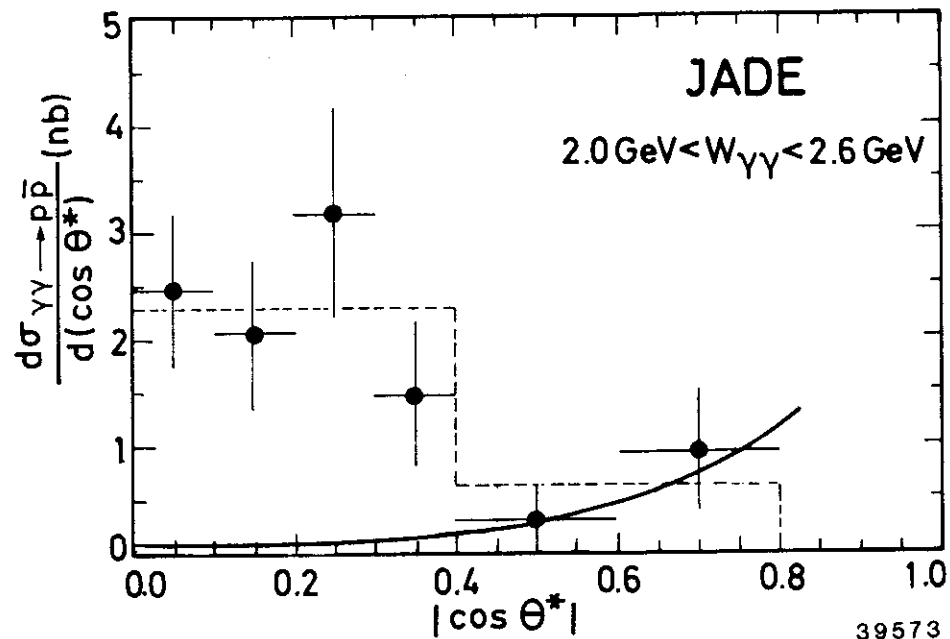


Fig. 4

39573